Smart Structures and Systems, *Vol. 32, No. 4 (2023) 219-233*
https://doi.org/10.12989/sss.2023.32.4.219

A fast and simplified crack width quantification method via deep Q learning

Xiong Peng, Kun Zhou, Bingxu Duan, Xingu Zhong*, Chao Zhao and Tianyu Zhang

[1] *Hunan University of Science and Technology, Taoyuan Road, Yuhu District, Xiangtan, China*
[2] *Hunan Provincial Key Laboratory of Structures for Wind Resistance and Vibration Control & School of Civil Engineering, Hunan University of Science and Technology, Taoyuan Road, Yuhu District, Xiangtan, China*

(*Received May 13, 2022. Revised April 12, 2023, Accepted September 26, 2023*)

Abstract. Crack width is an important indicator to evaluate the health condition of the concrete structure. The crack width is measured by manual using crack width gauge commonly, which is time-consuming and laborious. In this paper, we have proposed a fast and simplified crack width quantification method via deep Q learning and geometric calculation. Firstly, the crack edge is extracted by using U-Net network and edge detection operator. Then, the intelligent decision of is made by the deep Q learning model. Further, the geometric calculation method based on endpoint and curvature extreme point detection is proposed. Finally, a case study is carried out to demonstrate the effectiveness of the proposed method, achieving high precision in the real crack width quantification.

Keywords: concrete crack; crack width measurement; curvature extreme point; deep Q learning; geometric simplification

1. Introduction

Crack width is an important indicator for concrete structure health evaluation. In recent years, the crack recognition methods based on artificial intelligence and image processing has developed rapidly (Liu *et al*. 2014, Kim *et al*. 2017, Dorafshan *et al*. 2018, Bertelsen *et al*. 2019, Sony *et al*. 2021, Dais *et al*. 2021). Although the UAV or image acquisition platform provides convenient crack measurement approaches (Kim *et al*. 2017, Zhong *et al*. 2018, Jung *et al*. 2019, Ribeiro *et al*. 2020, Liu *et al*. 2020, Ali *et al*. 2021, Peng *et al*. 2021, Peng *et al*. 2021, Jang *et al*. 2021, Ji *et al*. 2021, Jiang *et al*. 2021), the crack width gauge carried by manual is still an important means in special or key area. As shown in Fig. 1, when the crack width gauge is used, the target area (0.4 cm × 0.3 cm) is enlarged for obtaining an 800 × 600 pixels image by amplification probe, and then the width is measured through a built-in program to represent the real crack width in this area. As shown in Fig. 1(d), when the manual mode is adopted, the probe is rotated and moved manually to make the scale suiting for crack edge; As shown in Fig. 1(e), if the crack measurement method based on extreme point detection is adopted, the edge of the crack is extracted by connecting two extreme points, and then the crack width is measured.

However, the accuracy of crack width measurement is related to the health condition evaluation of concrete structure, which has the following problems: (1) when the manual mode is adopted, the probe amplifier always needs to be moved and rotated, this process is time-consuming and laborious; (2) When the crack measurement method based on extreme point detection is adopted, the result is quite different from the manual measurement result shown in Fig. 1(e) with a relative error of about 45%. Therefore, it is of great significance to propose an automatic and accurate crack width calculation means. In this paper, we consider the crack width measurement as the decision-making process of position selection and geometric simplification mode, which is combining deep Q learning and geometric calculation.

2. Related work of crack recognition and width quantification

As a rapidly developing method, the Deep Learning may be applicable for recognizing a large amount of crack image data (Cha *et al*. 2017, Song *et al*. 2020). The target recognition network has applied to detect the ROI of cracks, which are divided into two categories: one-stage and two-stage network (Hu *et al*. 2021). To be specific, one-stage network such as SSD (Liu *et al*. 2016) and YOLO (Redmon and Farhadi 2018, Bochkovskiy *et al*. 2020), two-stage network such as Faster-RCNN (Girshick 2015) and R-FCN (Dai *et al*. 2016) are applied to crack detection (Deng *et al*. 2020, Park *et al*. 2020). These studies show that the deep learning method has good ability in crack classification and location. Then, in order to extract cracks, those pixel-level encoder to decoder networks such as FCN (Long *et al*. 2017), U-Net (Ronneberger *et al*. 2015, Choi and Cha 2019) and Deeplab (Chen *et al*. 2016, 2017) have applied to segment the crack (Ren *et al*. 2020, Ji *et al*. 2020, Kang *et al*. 2020). The application of deep learning method in crack recognition and segmentation improves the structure health assessment (Kang and Cha 2022).

*Corresponding author, Ph.D.,
E-mail: 1020086@hnust.edu.cn

ISSN: 1738-1584 (Print), 1738-1991 (Online)

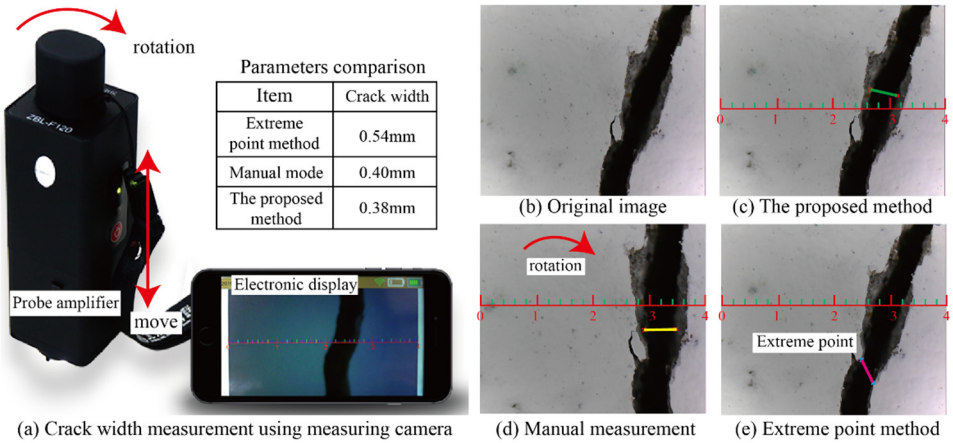

Fig. 1 Crack width measurement using width measuring camera

Further, the crack width can be used to evaluate safety state of structures effectively, which has attracted extensive attention of researchers. At present, there are three main methods of crack width calculation: flexible kernel method, center-line and physical formula. The crack width quantification method based on flexible kernel calculate the width of the kernel passing through the crack. Specifically, Lee proposed a shape-sensitive kernel within a semantic segmentation framework and a modified deep layer (Lee *et al*. 2020). Jin proposes the flexible kernel applied to calculate the propagation direction of the crack width, and its resolution is investigated according to the size of the kernel (Jin *et al*. 2020). Song proposed a width quantification method suitable for panorama cracks through crack matching and property calculation (Song *et al*. 2022); The center-line methods generate the center-line of the crack edge first, and then the width is quantified by measuring the distance of center-line and crack edges. To be specific, Jeremy proposed a novel hybrid method of crack width quantification by identifying a pair of points that give the shortest distance while being close to the orthogonal direction (Ong *et al*. 2022). Tang proposed an effective definition of crack width that combines the macro-scale and micro-scale characteristics of the backbone to obtain width. (Tang *et al*. 2023). Notably, Kang used modified distance transform method (DTM) to measure crack thickness and length in terms of pixel measurement, which has been achieved good accuracy (Kang and Cha 2022).

The crack width quantification method based on equation calculates crack width by specific physical equations. To be specific, Ni propose a Zernike-moment measurement of thin-crack width in images enabled by dual-scale deep learning. If the crack width W < 5 pixels, the ZM is the projections of the image data onto a set of complex polynomials, which form a complete orthogonal set over the interior of a unit circle to calculate the thin crack width (Ni *et al*. 2019). Wang propose new pavement crack width measurement method based on Laplace's equation. (Wang *et al*. 2018). Those methods have high accuracy and promote the development of crack width measurement.

However, the crack width quantification under the width-measuring instrument environment has some characteristics: (1) The amplification probe is used to amplify the 0.4 cm × 0.3 cm area to form an 800 × 600 pixels image. The crack features are magnified dozens of times. The correct measurement position should be selected and showed accurately, rather than measuring the width based on pointwise analysis. (2) The test environment is complex and changes greatly, but the geometric classification of crack edge is obvious.

The deep reinforcement learning is widely used in classification and decision-making problems because of its unique feedback mechanism (Mocanu *et al*. 2018, Liu *et al*. 2019, Liang *et al*. 2019, Yao *et al*. 2020). In this paper, we consider we consider the crack width quantification under the width-measuring instrument environment as a decision-making problem. Firstly, the U-Net network is used to segment the crack in pixel level, and the canny operator is applied to extract the crack edge. Then, the deep Q learning based on 4-layers neural network is constructed to form the intelligent decision model. Further, the fast crack width quantification method is proposed based on geometric simplification through endpoint and curvature maximum point detection. Finally, the usefulness of this method is demonstrated in a case study compared with existed methods, which can achieve about 90% accuracy in crack width measurement.

3. Methodology

In order to calculate the crack width reliably and accurately, we have proposed a new method combining deep learning and reinforcement learning, as shown in Fig. 2, which will be introduced in the following sections. This framework including three main tasks: (1) crack image preprocessing; (2) width measurement position decision; (3) crack width calculation.

3.1 Crack image preprocessing

The crack width measurement based on width-measuring instrument that amplify the 0.4 cm × 0.3 cm area to form an 800 × 600 pixels image. The crack features are magnified dozens of times, which are obviously different

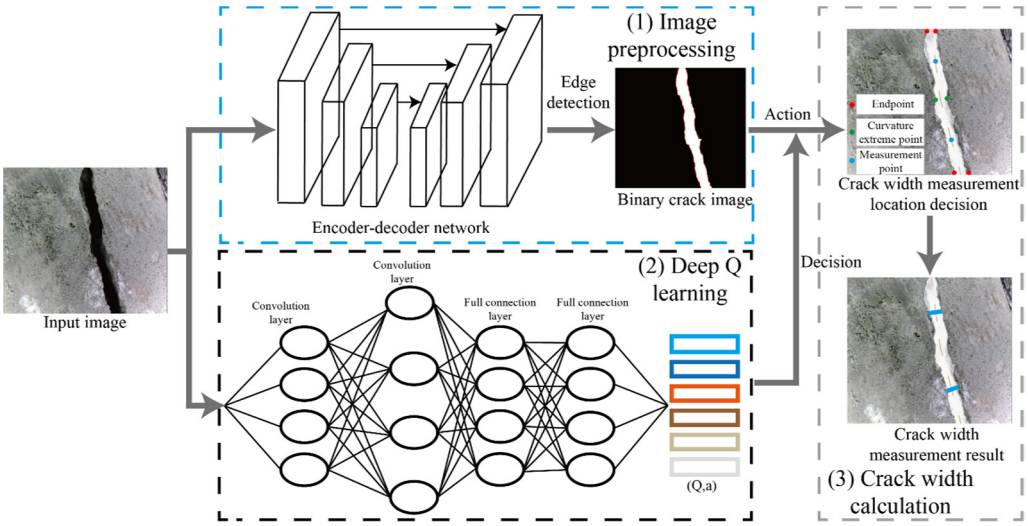

Fig. 2 Framework of crack width measurement based on deep Q learning

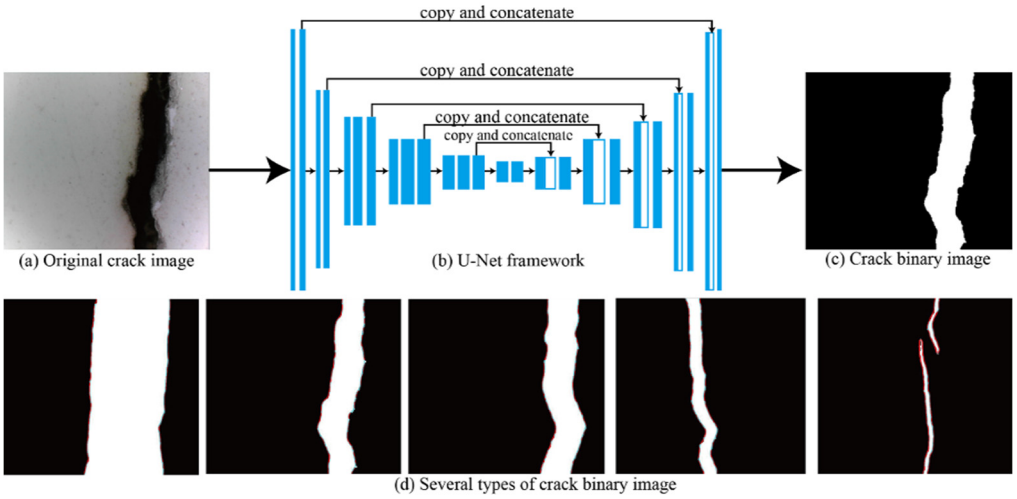

Fig. 3 The preprocessing of crack image

from noises such as watermark or imprint. As shown in Fig. 3, the crack is segmented by U-Net network for image preprocessing. The U-Net is originally proposed by Ronneberger *et al* (2015). This network applies the jump connection to image segmentation, which greatly improves its accuracy. Its encoder includes three steps, and each step includes two 3 × 3 convolution layer and a 2 × 2 convolution layer with stride = 2. After the convolution operation, the multiple feature maps are output, the size of the feature map is reduced by each maximum pool layer twice. The number of feature maps output in the three steps are 16, 32 and 64 respectively, and the size is respectively 64 × 64, 32 × 32, 16 × 16. Compared with the encoding process, the feature decoding process also includes three steps. Each step first performs an upsampling operation with a 2 × 2 convolution layer with stride = 2 on the feature map from the lower level, then cascade with the feature map of the left encoder part, and finally the feature map is output through two 3 × 3 convolutions.

The binary crack image shown in Fig. 3(b) is obtained by U-Net model. Then, the edge of binary crack image is detected by Canny operator, which is fused with the original binary image to form preprocessing results shown in Fig. 3(c). As shown in Fig. 3(d), the clear edges of several types crack are obtained after preprocessing.

3.2 Crack width measurement position decision

3.2.1 Overview of deep Q learning

The reinforcement learning is the representative of behaviorism artificial intelligence, which is applied to describe the interaction process of maximizing the strategy learning reward between agent and environment (Mnih *et al*. 2005). And the deep reinforcement learning is formed by the complementary combination of deep learning and reinforcement learning, which has strong feature extraction and decision-making ability (Wiering *et al*. 2011, Mnih *et al*. 2013). The problem model is usually represented as a tuple $[S, A, T, r]$, where S represents the state space, A represents the action, and $T\{s, a, s'\} \rightarrow [0,1]$ is the state transition function, representing the probability of switching to another state S' after performing an action in state s. And

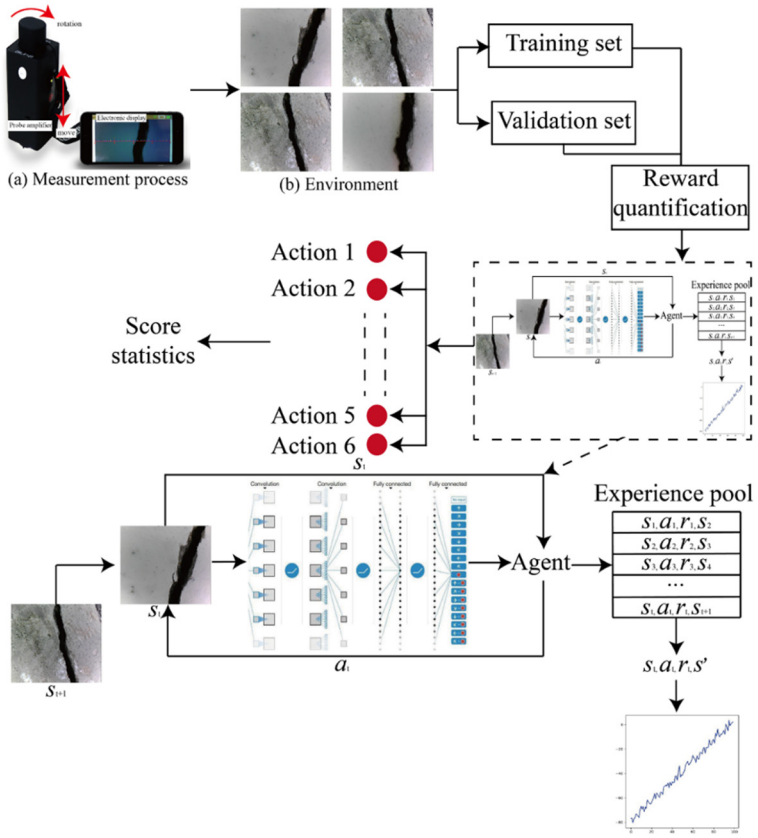

Fig. 4 The crack image classification process based on deep Q learning

r is the reward function, which represents the feedback obtained from the environment when the state transition occurs. Through repeated interactions with the environment, the value function is continuously trained and updated based on the obtained information, and finally the optimal strategy is well-trained. The iterative update equation of the function Q is as follows

$$Q_{t+1}(S_t, a_t) = Q_t(S_t, a_t) + \alpha\delta_t \tag{1}$$

Where α is the learning rate, δ_t represents the time difference error, and is expressed as Eq. (2)

$$\delta_t = r_{t+1} + \gamma Q_t(S_{t+1}, \alpha') - Q_t(S_t, \alpha_t) \tag{2}$$

Where α' is the action that can be executed in the state S_{i+1}. As shown in Fig. 4, when the crack width measuring-instrument is applied in the real environment, the test environment changes greatly, so it has high requirements for robustness and fault tolerance. Therefore, we have proposed a crack geometry classification method based on deep Q learning, the crack image data collected by width-measuring instrument that is regarded as the environmental state S. And the classification of the corresponding geometric operation is regarded as action α. The reward function R is established based on the corresponding relationship between the crack geometry classification results and ground-truth labels.

3.2.2 Deep Q learning architecture

The classical Q learning is a tabular method, which has the problem of dimension disaster in high-dimensional state environment space or continuous state space. Due to the strong representation ability of deep learning, the deep crack feature is extracted by the 4-layers network shown in Fig. 5(a), which is fused with the full connection layer using one-shot mechanism. And then the corresponding Q value shown in Fig. 5(b) is output. This architecture includes two neural networks, which are the estimated value network of updating neural network parameters and the target value network of updating Q value. These two networks have the same structure, and the DQN uses the deep neural network with parameter θ to approximate the action value function as Eq. (3)

$$Q(s, \alpha'; \theta) \approx Q_\pi(s, \alpha) \tag{3}$$

During the training, the parameters are updated by minimizing the loss function

$$L_t(\theta_t) = E_{(s,\alpha,r,s')}[(y - Q(s, \alpha'; \theta_t))^2] \tag{4}$$

Where L_t is the loss function at time of t; θ_t is the parameter of Q network at time of t; E indicates mathematical expectation; and y is the optimization target value of Q network in the Eq. (5)

$$y = r + \gamma Q(s', \alpha'; \theta_t^-) \tag{5}$$

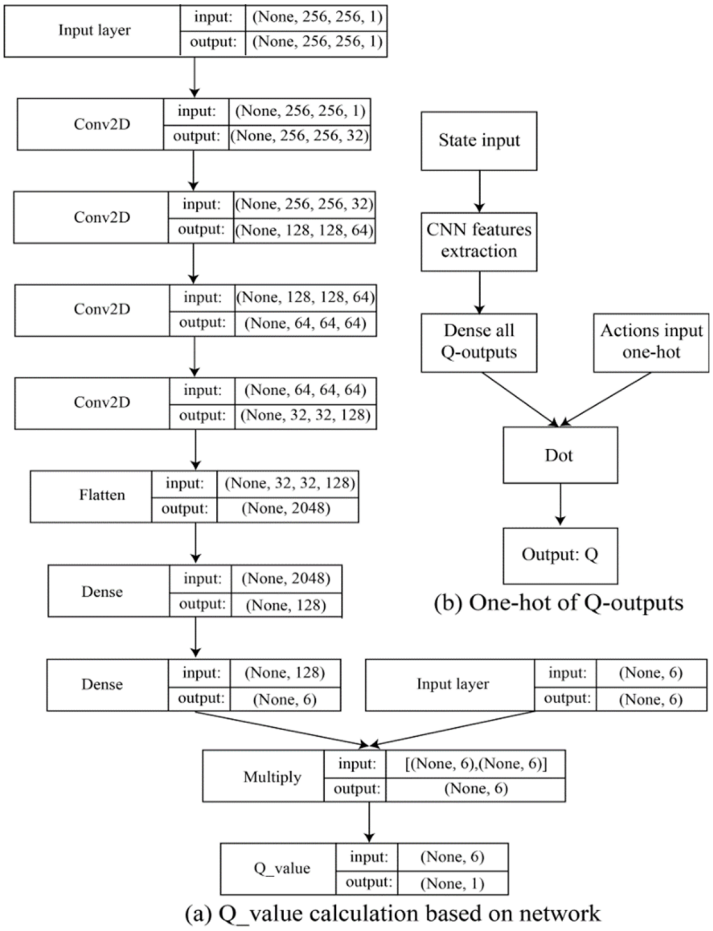

Fig. 5 The process of Q-output based on CNN network

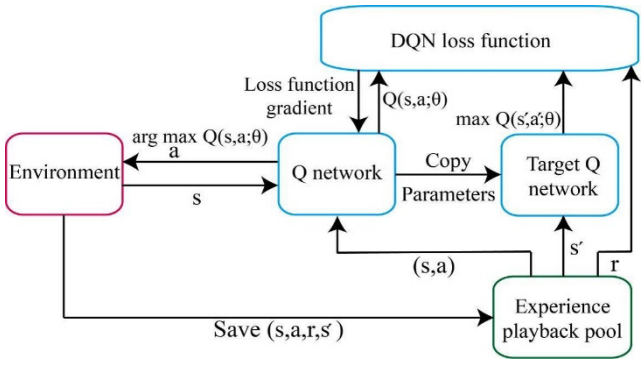

Fig. 6 The algorithm architecture of deep Q learning

Where θ_t^- is the parameter of the target network, and the weight of deep Q network is updated based on gradient rule, and the weight of partial derivative can be obtained by the loss function in Eq. (6)

$$\nabla_{\theta_t} L_t(\theta_t) = E_{(s,\alpha,r,s')}[(y - Q(s,\alpha;\theta_t)\nabla_{\theta_t} Q(s,\alpha;\theta_t] \quad (6)$$

Where ∇ represents gradient calculation. Through experience playback mechanism, the tuple composed of experience, action and reward of the agent is stored to form a memory sequence $(s_t, \alpha_t, r, s_{t+1})$. During training, a small batch of experience is randomly extracted from the experience playback pool each time, and then the network parameters are updated according to the random gradient descent method.

3.3 Crack width quantification

In order to calculate the crack width quickly and accurately, the fast simplified quantification method is proposed by endpoint and curvature maximum point detection. The crack width calculation process is mainly divided into (1) Crack edge shape simplification; (2) Crack width calculation.

3.3.1 Crack edge shape simplification

(1) Curvature extreme point detection

The linear curvature of the crack edge is calculated as Eqs. (7)-(8), and the curve is expressed as a parametric equation of arc length μ shown in Fig. 7(c)

$$L(\mu) = (x(\mu), y(\mu)) \quad (7)$$

The expression of curve variation with scale is

$$L_\sigma = (x(\mu,\sigma), y(\mu,\sigma)) \quad (8)$$

Where x and y are the abscissa and ordinate of the points on the contour curve respectively, and x and y are one-dimensional functions. Of which

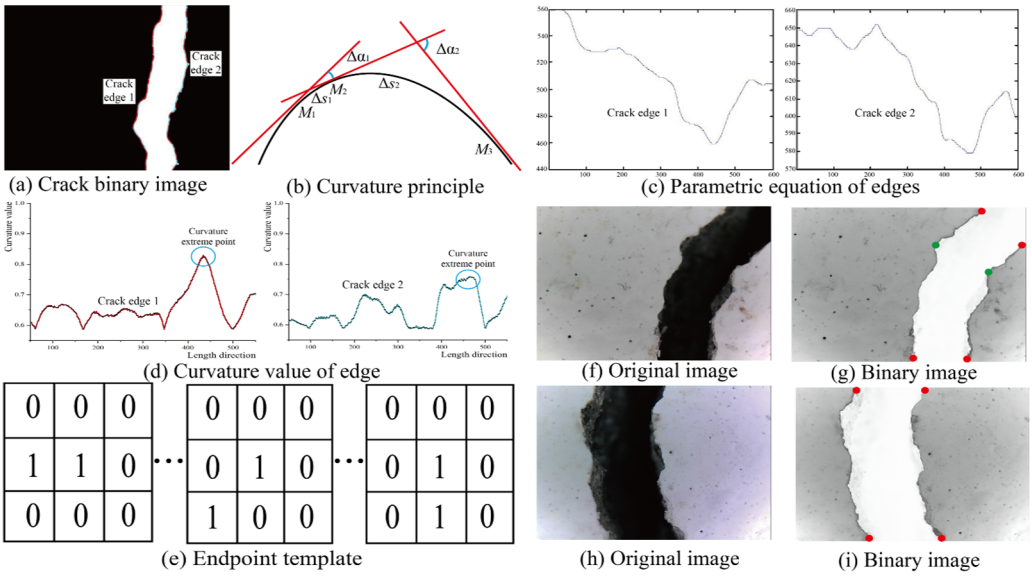

Fig. 7 Simplification of crack edge shape

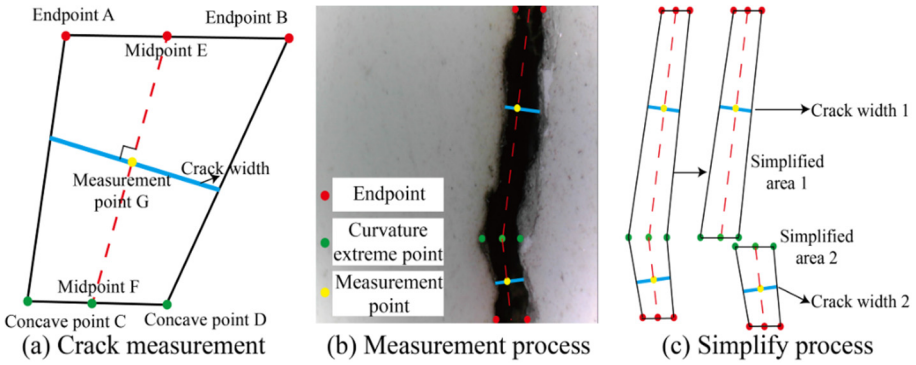

Fig. 8 Crack width calculation based on geometry simplification

$$X(\mu,\sigma) = x(\mu) * g(\mu,\sigma) \tag{9}$$

$$Y(\mu,\sigma) = Y(\mu) * g(\mu,\sigma) \tag{10}$$

Then the curvature k can be expressed as

$$k(\mu,\sigma) = \frac{X_\mu(\mu,\sigma)Y_{\mu\mu}(\mu,\sigma) - X_{\mu\mu}(\mu,\sigma)X_\mu(\mu,\sigma)}{\sqrt{(X_u(\mu,\sigma)^2 + Y_u(\mu,\sigma)^2)^3}} \tag{11}$$

$g(\mu,\sigma)$ represents the Gaussian function of scale σ in the target image; σ represents the width parameter of the Gaussian function. The curvature of all points on the crack edge is calculated shown in Fig. 7(a) and the curvature distribution curve is formed shown in Fig. 7(d).

(2) Geometry simplification

Firstly, the endpoints are detected based on template operator shown in Fig. 7(e), and a series of concave points are formed after calculating the local extreme points shown in Fig. 7(g) and (i). The following concave filtering methods are defined:

1) Determine the curvature extreme points in the two edge connected domains;

2) According to the reinforcement learning classification results, the number of clustering centers are determined as N, is found by traversing all curvature points except the maximum point, and the distance from the maximum point is calculated, and keep the store if the distance value is greater than 30. Repeat the above steps until the number of curvature extreme points is equal to the number of cluster centers. The final curvature filtering result is shown in Fig. 7(d);

3) After the concave extreme point is detected, it is sorted according to the spatial relationship, and the extreme points in the corresponding order are connected. The matched concave points are connected to complete the geometric simplification and reconstruct the crack image shown in Figs. 7(g) and (i), which provides a basis for crack width calculation.

3.3.2 Crack width calculation

In order to realize measuring crack width automatically and accurately, after geometric simplification, the simplified crack edge shape is decomposed into quadrilateral graphic combination. As shown in Fig. 8(a), the coordinates of the quadrilateral after concave point matching are $A(x_0, y_0)$, $B(x_1, y_1)$, $C(x_2, y_2)$, $D(x_3, y_3)$, and the coordinates of the

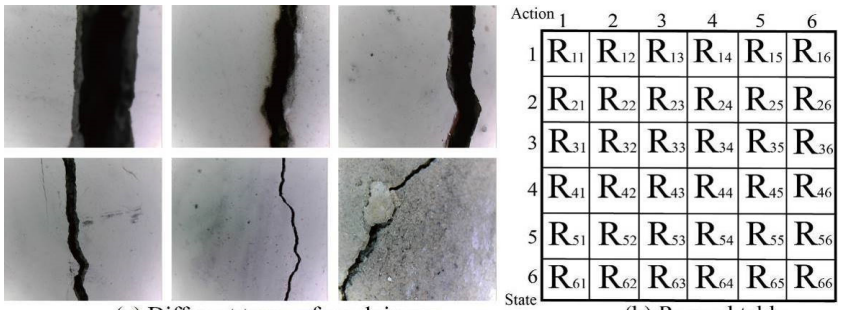

(a) Different types of crack image (b) Reward table

Fig. 9 Reward value table of crack classification

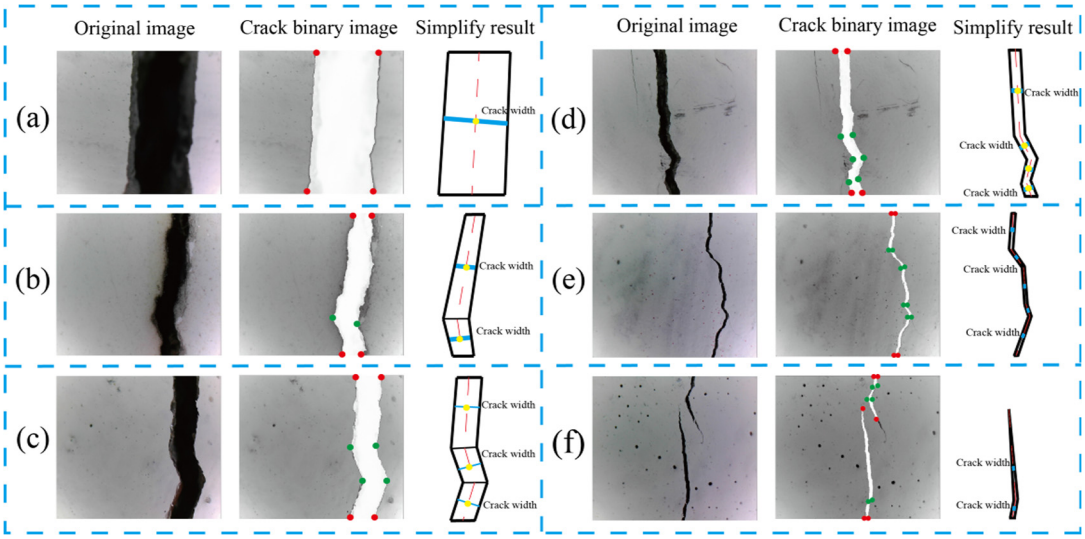

Fig. 10 Simplify results of different classification type

measurement point G of the quadrilateral $ABCD$ are

$$x_g = \frac{x_0 + x_1 + x_3 + x_4}{4} \tag{12}$$

$$y_g = \frac{y_0 + y_1 + y_3 + y_4}{4} \tag{13}$$

Make a vertical line l through point $G(x_g, y_g)$, which is defined as the approximate width in this area

$$y = \frac{x_3 + x_4 - x_1 - x_2}{y_1 + y_2 - y_3 - y_4}(x - x_g) + y_g \tag{14}$$

Finally, the width is defined as the distance between the intersection of vertical line l shown in Fig. 8(c).

3.4 Reward function

The goal of reinforcement learning is to maximize the reward, and the reward function defines the value obtained by agents performing different behaviors in the current environment. R_s is the reward function, which represents the reward expectation when the state transition occurs at a certain time t in s state, which is defined as Eq. (15).

$$R_s = E[R_{t+1}|S_t = s] \tag{15}$$

And the total reward function is calculated as Eq. (16)

$$G_t = R_{t+1} + \gamma R_{t+2} + \cdots = \sum_{k=0}^{\infty} \gamma^k R_{t+k+1} \tag{16}$$

Among them, the attenuation coefficient γ reflects the value proportion of future rewards at the current moment. The setting of reward function will affect the update speed and the generalization ability of algorithm. As shown in Fig. 9, the cracks are classified according to the distribution state of edge curvature, and the reward function R_{ij} is defined based on the classification result. As shown in Fig. 10, these different types of cracks are simplified according to classification results.

4. Case study

In this paper, we have developed a novel crack width quantification method based on deep Q learning. In order to verify the effectiveness of the proposed method, a case study using crack width gauge are carried out. The proposed method is trained and tested by the collected image data, and the tested result is compared with the well-known methods in detection accuracy and time-cost. As shown in Fig. 11, the crack width gauge is applied to collect bridge

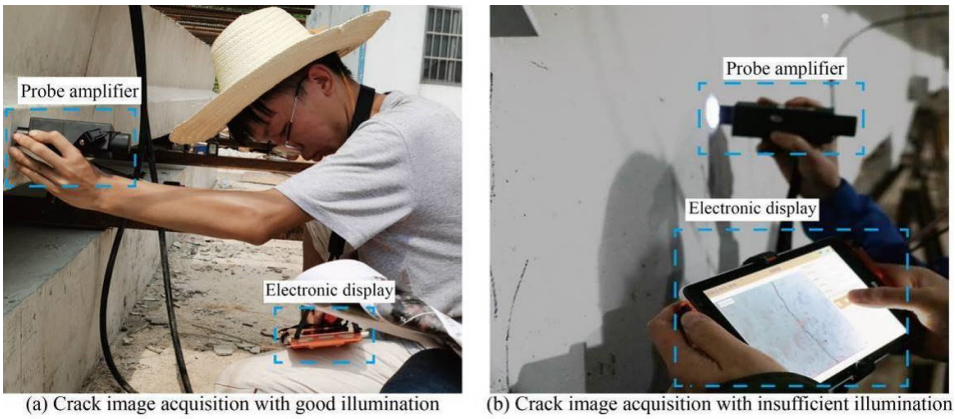

(a) Crack image acquisition with good illumination (b) Crack image acquisition with insufficient illumination

Fig. 11 Crack data acquisition based on ZBL crack measuring camera

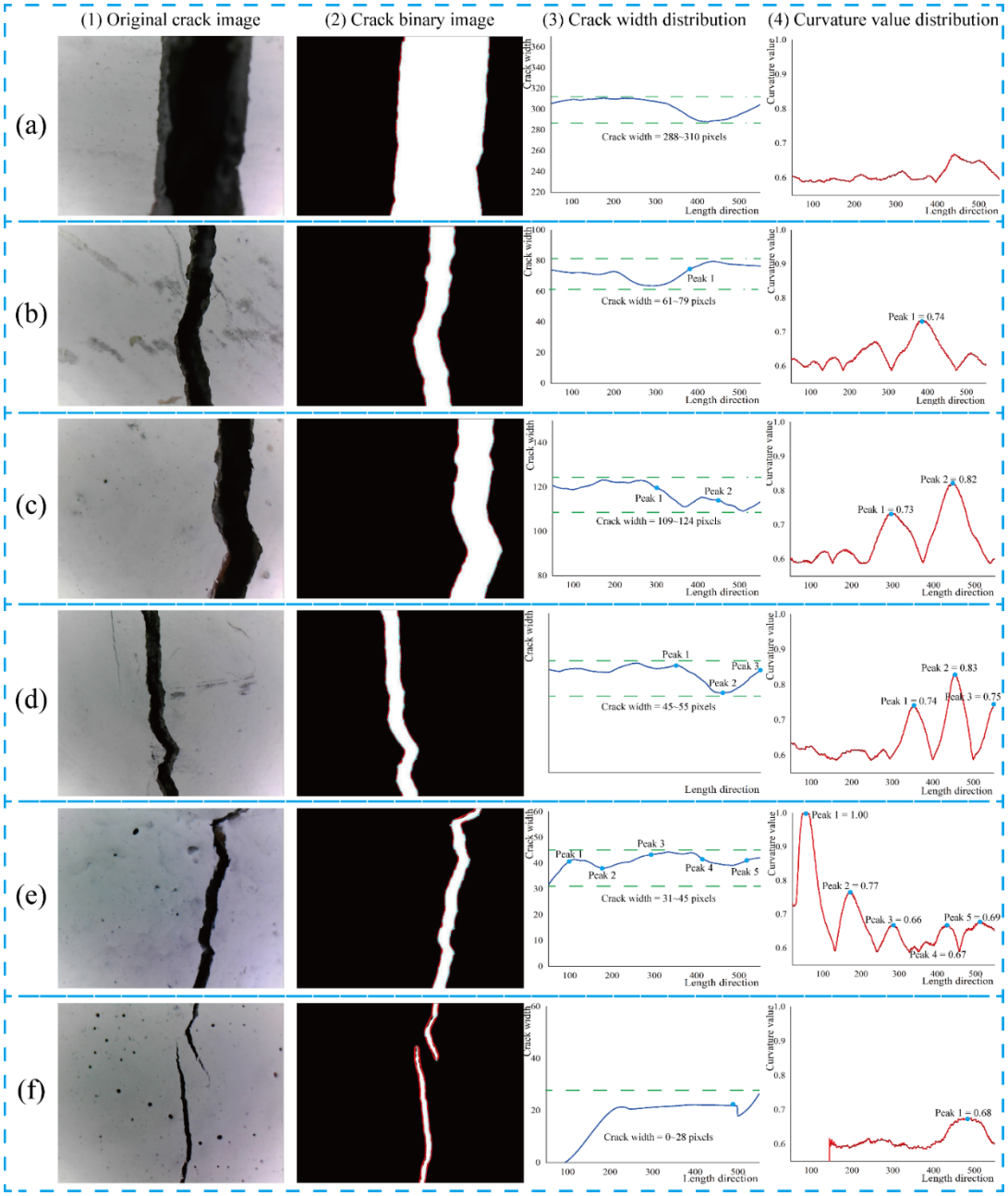

Fig. 12 Curvature value of crack edge

Table 1 The classification data set of concrete cracks

Items	Images size	Training	Validation	Total
Classification 1 (0 curvature extreme point)	800×600	128	32	160
Classification 2 (1 curvature extreme point)	800×600	280	70	350
Classification 3 (2 curvature extreme point)	800×600	184	46	230
Classification 4 (3 curvature extreme point)	800×600	144	36	180
Classification 5 (≧ 4 curvature extreme points)	800×600	392	98	490
Classification 6 (Special conditions)	800×600	320	80	400

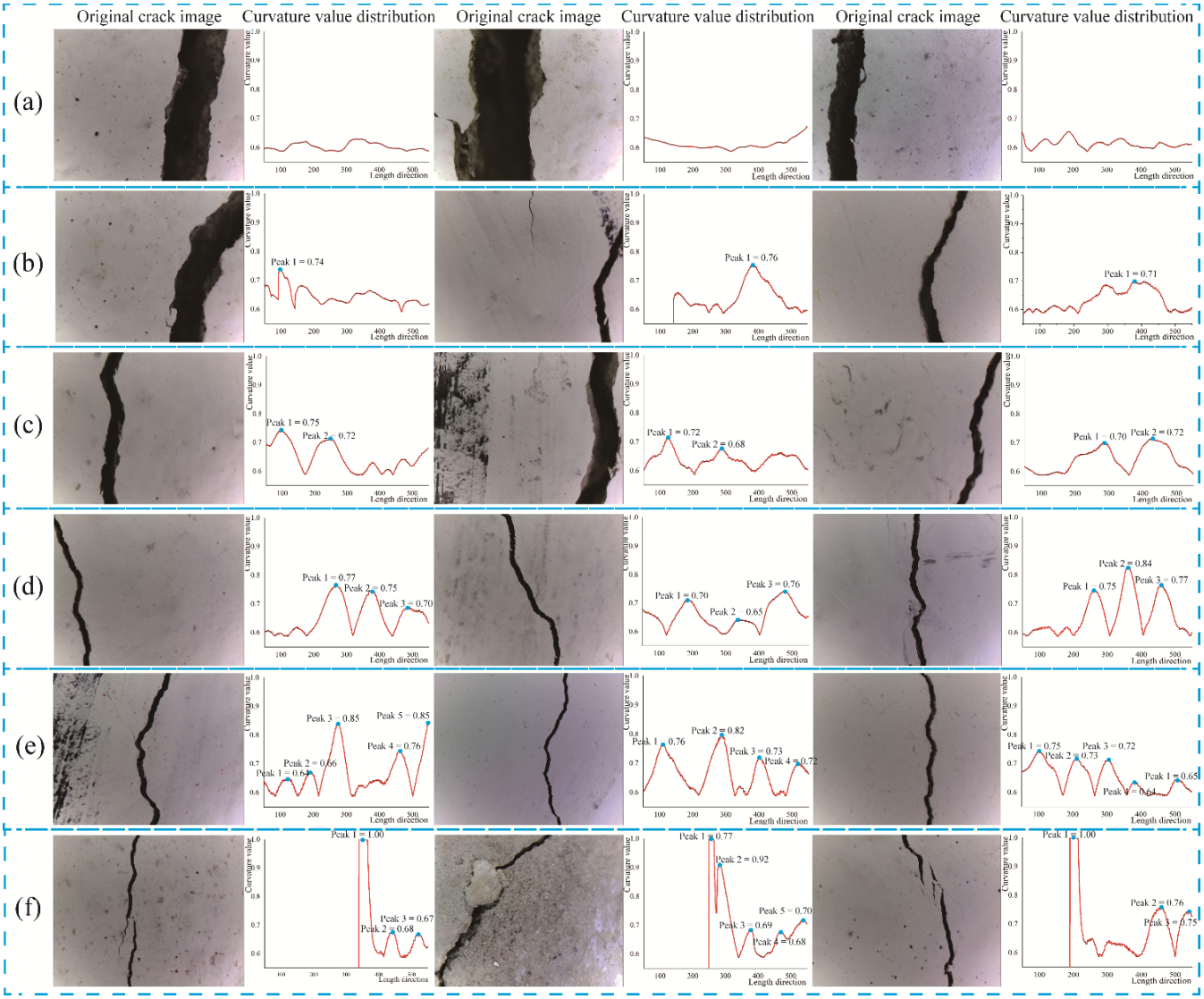

Fig. 13 Samples of crack data set; (a) 0 curvature extreme point; (b) 1 curvature extreme point; (c) 2 curvature extreme point; (d) 3 curvature extreme point; (e) ≧ 4 curvature extreme point; (f) 5 special conditions

crack data with good or insufficient illumination.

4.1 Data set build

In order to training the model of crack width recognition based on deep reinforcement learning, the crack image data set is established. The edges of crack image are detected based on previous method shown in Fig. 12(2), and the curvature value is calculated along the crack boundary shown in Fig. 12(4). The cracks width along the crack boundary point are obtained by manual shown in Fig. 12(3). The crack edge distribution has obvious characteristics, and the change of crack width is consistent with the change of curvature value shown in Figs. 12(a)-(f). It shows that when the curvature of crack edge is within a specific range, the crack width changes little in this range, and this vertical

width can represent the average width. Therefore, we have classified the crack dataset images according to the curvature distribution of the crack edge. Taking 0-4 pairs of curvature extreme points as the crack classification basis, a total of 5 common types and a special type of crack are formed (600 × 800 pixels) shown in Figs. 13(a)-(f). There are 1810 images in total, according to the ratio of the training set to test set to verification set to = 4:1, the image data are divided into the training data set (1448) and test data set (362) shown in Table 1.

4.2 Training and evolution

The reinforcement learning is trial-and-error learning based on behaviorism. The initial training process of the model can be regarded as random guess. The number of steps is defined in each epoch, and the trial-and-error interaction are carried out in each step. At each step, the agent obtains an action a from the actor based on the ϵ-greedy algorithm, and then the next state and reward is obtained using uses the action to interact with the environment. This experience would be added to memory, then the memory would be play back to update the critical parameters. The parameters of critic network are copied to actor network, and the total return and loss of each epoch are monitored. According to the strong mapping relationship between the crack edge geometric shape and the change of crack normal width, the reward function is defined as Eq. (17)

$$R(s_i, \alpha_i, y_i) = \begin{cases} +1, & \alpha_i = y_i \\ -1, & \alpha_i \neq y_i \end{cases} \tag{17}$$

In the training process, the exploration probability ε decays from 1.0 to 0.01 according to Eq. (18)

$$\varepsilon = \max\left\{\varepsilon_{min}, 1 - \frac{(1-\varepsilon_{min}) \times step}{total}\right\} \tag{18}$$

Where step is the current number of iterations, total is the number of iterations. Exploration rate $\gamma = 0.99$, plot k = 100, the number of iterations is 5000, and the mean scores are calculated in a group of 10 points shown in Fig. 14(b). At the beginning, the reinforcement learning model is a random guess, so the initial total score is about -80. The 100 samples are played back in the experience pool every iteration of the model. When the DQN model is trained reaching 2000 times, the model converges well, the reward value is concentrated at about 90, indicating that the accuracy of crack classification prediction is about 90% shown in Fig. 14(b).

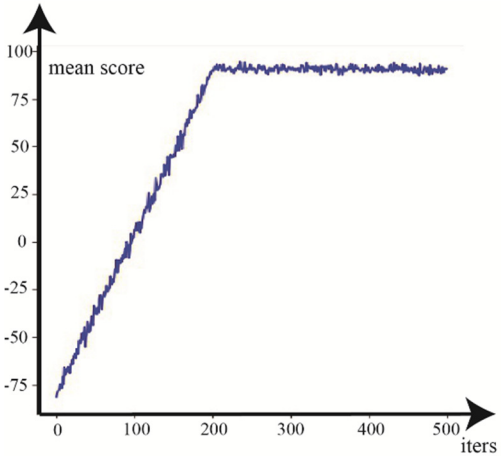

Fig. 14 Training reward curve

4.3 Algorithm implementation

According to the proposed method, the detail process of crack width measurement is shown in Fig. 15. Firstly, the

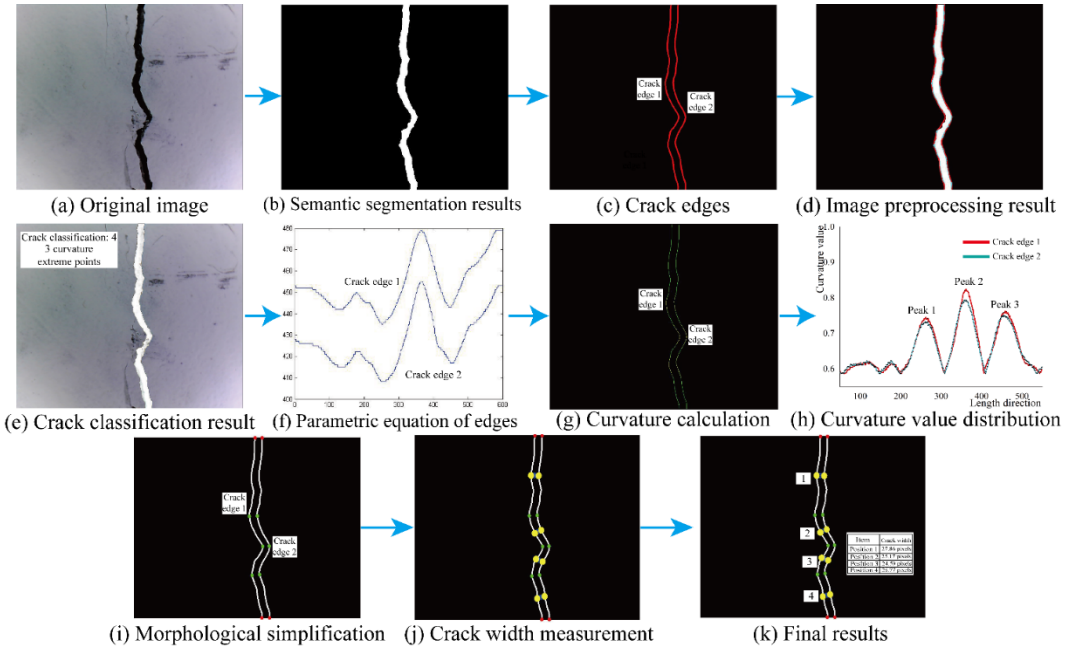

Fig. 15 The detail process of crack width measurement

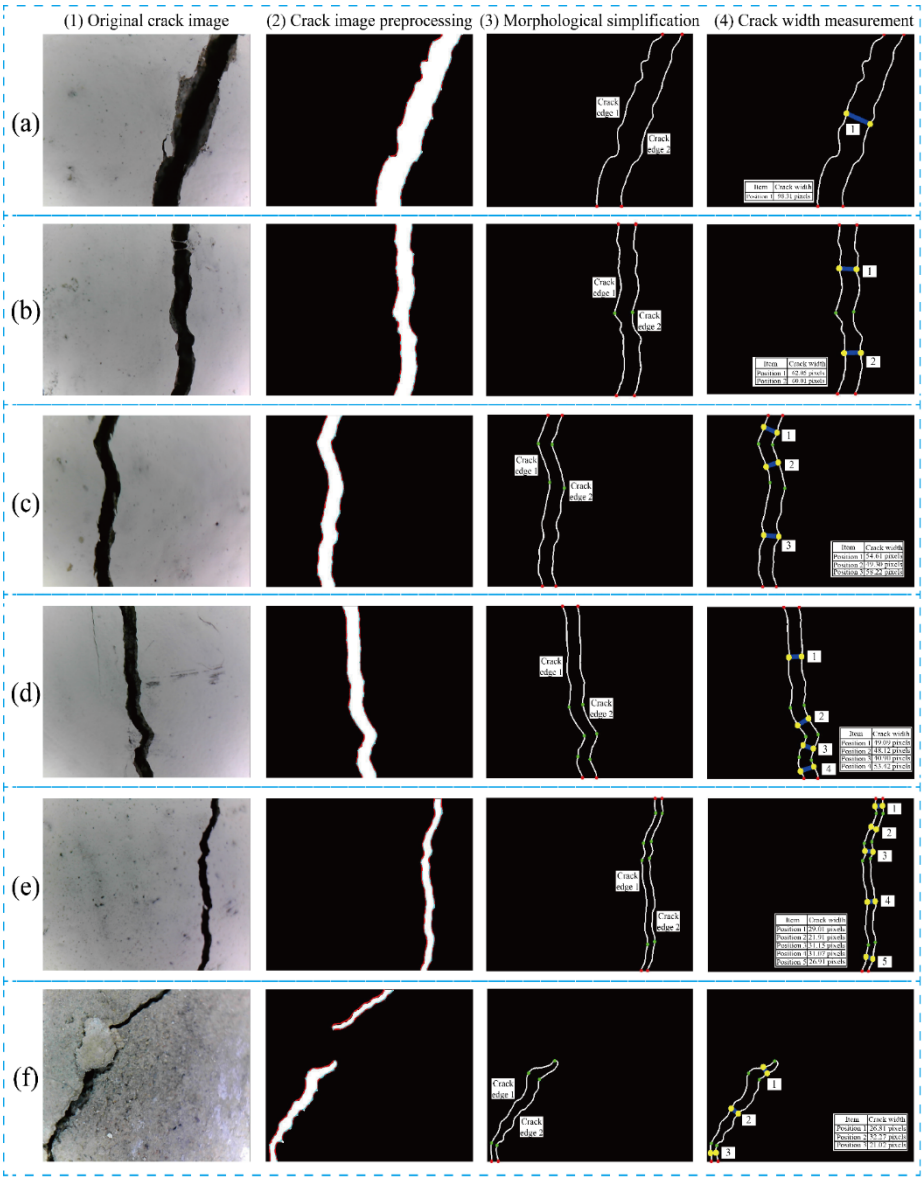

Fig. 16 The crack width measurement process of the proposed method; (a) 0 curvature extreme point; (b) 1 curvature extreme point; (c) 2 curvature extreme point; (d) 3 curvature extreme point; (e) ≧ 4 curvature extreme point; (f) special conditions

original crack image (800×600 pixels) shown in Fig. 15(a) is segmented by the well-trained U-Net network in pixel level shown in Fig. 15(b). Then, the edges of binary crack are detected by Canny operator with the Gaussian filter value of 8 shown in Fig. 15(c). Finally, the preprocessing result of crack image are fused with semantic segmentation result shown in Fig. 15(d). On the other hand, the original crack image is classified as action 3 by the trained reinforcement learning model shown in Fig. 15(e). The edge of the crack is transformed into a parametric equation, and the curvature of each point on the edge is calculated according to section 3.3.1 shown in Figs. 15(f) and (g). According to the classification results of well-trained model, three pairs of extreme points on the curvature coordinate curve are matched shown in Figs. 15(h) and (i). Finally, the geometric simplification of Fig. 15(i) is carried out and the measurement position is obtained. The corresponding crack width is calculated shown in Fig. 15(k). And the crack widths with typical classification features is calculated shown in Fig. 16.

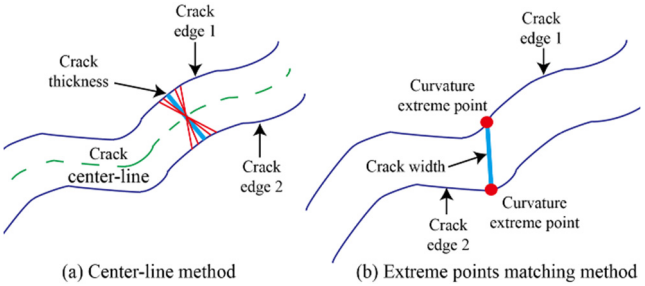

Fig. 17 Comparison method of crack width measurement

Table 2 Comparison of crack width measurement result for proposed method, ground-truth, center-line method and extreme point method

Item	Condition 1	Condition 2	Condition 3	Condition 4	Condition 5	Condition 6
Proposed method	98.31	62.05	58.22	53.42	31.15	32.27
Ground truth	102.83	66.19	57.29	56.27	32.98	35.72
Center-line method	108.65	64.03	58.27	59.23	35.04	45.61
Extreme point method	164.49	148.73	71.69	63.25	45.27	46.44

Table 3 Comparison of average accuracy parameters for proposed method, center-line method and extreme point method

Methods	Average accuracy	Time (s)
Proposed method	94.58%	1.76
Center-line method	92.85%	6.56
Extreme point method	67.57%	1.23

4.4 Algorithm performance comparison

In order to verify the effectiveness of this method for crack width measurement, the center-line method and the extreme point matching method are used for comparative experiments shown in Fig. 17 (Shan *et al*. 2015, Payab *et al*. 2018). In Fig. 17(a), the centerline is obtained by the classical skeleton extraction algorithm (Zhou and Liu 2019). And the ground-truth is based on manual measurement in original crack image. The crack thickness is defined as the distance between the intersection of the vertical line and the edge shown in Fig. 17(b).

To evaluate the performance of these methods quantitatively, the 100 test images formed the data set concluding 6 categories are inputted into the framework shown in Fig. 16. The evaluation results are shown in Table 2 and Fig. 18. Compared with the other two methods, this method has higher accuracy and less time cost shown in Table 3. As shown in Fig. 18(2), the proposed method has a good effect in six different conditions, but the extreme point matching method has a large error in the measurement accuracy.

As shown in Fig. 16(f) and Table 2 (condition 6), there is a large width area in this crack, the centerline method directly defines the widest part of the centerline-width as the crack width, which has some errors with the manual measurement. However, the proposed method considers the distribution of crack curvature, thus the distribution of crack width is considered, it is consistent with the actual manual measurement result.

On the other hand, although the centerline method also has high accuracy, it cannot directly display the position of the measurement point. The centerline algorithm adopts iterative method to obtain robust centerline, and its time cost is as high as 6.56 s, so it is not suitable for a built-in method of instrument. Therefore, the proposed method has high accuracy and fast calculation speed, which can be used in crack width measuring instrument.

5. Conclusions

In this paper, we have proposed a fast and simplified quantification crack width method via deep Q learning. The following findings and conclusions are offered:

- Based on the statistics of concrete crack data set, a geometric simplified model for crack width calculation is proposed. The crack width measurement process is regarded as the geometric simplification of the crack edge, which not only meets the accuracy requirements of practical engineering measurement, but also greatly reduces the time cost.
- Aiming at the complexity and diversity of concrete crack images, the crack image classification method based on deep Q learning is proposed. Based on the geometric information statistical results of crack edge, the cracks are divided into 6 categories. Compared with center-line method and extreme point method network, the proposed method has higher extraction and less time cost in crack width calculation. The usefulness of this method is demonstrated in a case study compared with existing methods, which can achieve about 90% accuracy in crack width measurement. The time cost of the proposed method is about 1.76 s per one 800 × 600 pixels image.

Acknowledgments

This study is supported by National Natural Science Foundation of China (Grant No. 51678235) and the Natural Science Foundation of Hunan Province (2020JJ5195), to which the authors are grateful.

References

Ali, R., Kang, D., Suh, G. and Cha, Y.J. (2021), "Real-time multiple damage mapping using autonomous UAV and deep faster region-based neural networks for GPS-denied structures", *Automat. Constr.*, **130**(2), 103831. https://doi.org/10.1016/j.autcon.2021.103831

Bertelsen, I.M.G., Kragh, C., Cardinaud, G., Ottosen, L.M. and Fischer, G. (2019), "Quantification of plastic shrinkage cracking in mortars using digital image correlation", *Cement Concrete Res.*, **123**, 105761. https://doi.org/10.1016/j.cemconres.2019.05.006

Bochkovskiy, A., Wang, C.Y. and Liao, H.Y.M. (2020), "Yolov4: Optimal speed and accuracy of object detection", *arXiv preprint*

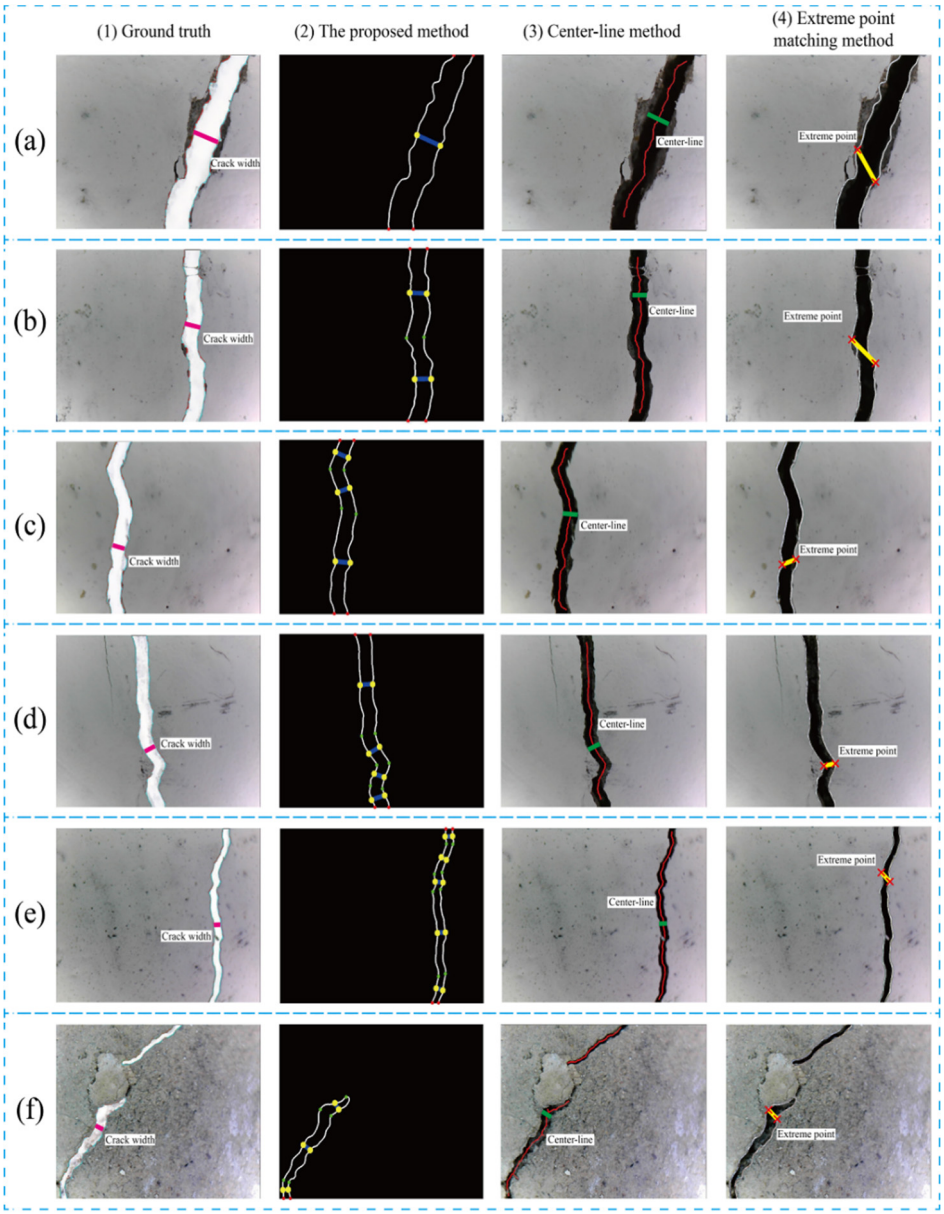

Fig. 18 Comparison of crack width measurement results with different conditions; (a) 0 curvature extreme point; (b) 1 curvature extreme point; (c) 2 curvature extreme point; (d) 3 curvature extreme point; (e) ≧ 4 curvature extreme point; (f) special conditions

arXiv:2004.10934, 2020. https://doi.org/10.48550/arXiv.2004.10934

Cha, Y.J., Choi, W. and Büyüköztürk, O. (2017), "Deep learning-based crack damage detection using convolutional neural networks", *Comput. Aided Civil Infrastr. Eng.*, **32**(5), 361-378. https://doi.org/10.1111/mice.12263

Chen, L.C., Papandreou, G., Kokkinos, I., Murphy, K. and Yuille, A.L. (2016), "Deeplab: Semantic image segmentation with deep convolutional nets, atrous convolution, and fully connected crfs", *IEEE Transact. Pattern Anal. Mach. Intell.*, **40**(4), 834-848. https://doi.org/10.1109/TPAMI.2017.2699184

Chen, L.C., Papandreou, G., Schroff, F. and Adam, H. (2017), "Rethinking atrous convolution for semantic image segmentation", *arXiv preprint arXiv:1706.05587*. https://doi.org/10.48550/arXiv.1706.05587

Choi, W. and Cha, Y.J. (2019), "SDDNet: Real-time crack segmentation", *IEEE Transact. Industr. Electron.*, **67**(9), 8016-8025. https://doi.org/10.1109/TIE.2019.2945265

Dai, J., Li, Y., He, K. and Sun, J. (2016), "R-FCN: Object detection via region-based fully convolutional networks", *Adv. Neural Inform. Process. Syst.*, **2016**, 29.

Dais, D., Bal, I.E., Smyrou, E. and Sarhosis, V. (2021), "Automatic crack classification and segmentation on masonry surfaces using convolutional neural networks and transfer learning", *Automat. Constr.*, **125**(4), 1-18. https://doi.org/10.1016/j.autcon.2021.103606

Deng, J., Lu, Y. and Lee, V.C.S. (2020), "Imaging-based crack detection on concrete surfaces using You Only Look Once network", *Struct. Health Monitor.*, **20**(2), 147592172093848.

Dorafshan, S., Thomas, R.J. and Maguire, M. (2018), "Comparison of deep convolutional neural networks and edge detectors for image-based crack detection in concrete", *Constr. Build. Mater.*, **186**, 1031-1045. https://doi.org/10.1016/j.conbuildmat.2018.08.011

Gehri, N., Mata-Falcón, J. and Kaufmann, W. (2020), "Automated crack detection and measurement based on digital image correlation", *Constr. Build. Mater.*, **256**, 119383. https://doi.org/10.1016/j.conbuildmat.2020.119383

Girshick, R. (2015), "Fast R-CNN", *IEEE International Conference on Computer Vision*, Santiago, Chile, December, pp. 1440-1448.

Guo, L., Li, R., Jiang, B. and Shen, X. (2020), "Automatic crack distress classification from concrete surface images using a novel deep-width network architecture", *Neurocomput.*, **397**, 383-392. https://doi.org/10.1016/j.neucom.2019.08.107

Hu, W., Wang, W., Ai, C., Wang, J., Wang, W., Meng, X., Liu, J., Tao, H. and Qiu, S. (2021), "Machine vision-based surface crack analysis for transportation infrastructure", *Automat. Constr.*, **132**, 103973. https://doi.org/10.1016/j.autcon.2021.103973

Jang, K., An, Y.K., Kim, B. and Cho, S. (2021), "Automated crack evaluation of a high-rise bridge pier using a ring-type climbing robot", *Comput.-Aided Civil Infrastr. Eng.*, **36**, 14-29. https://doi.org/10.1111/mice.12550

Ji, A., Xue, X., Wang, Y., Luo, X. and Xue, W. (2020), "An integrated approach to automatic pixel-level crack detection and quantification of asphalt pavement", *Automat. Constr.*, **114**, 103176. https://doi.org/10.1016/j.autcon.2020.103176

Ji, A., Xue, X., Wang, Y., Luo, X. and Wang, L. (2021), "Image-based road crack risk-informed assessment using a convolutional neural network and an unmanned aerial vehicle", *Struct. Control Health Monitor.*, **28**(7), p. e2749. https://doi.org/10.1002/stc.2749

Jiang, Y., Han, S. and Bai, Y. (2021), "Building and infrastructure defect detection and visualization using drone and deep learning technologies", *J. Perform. Constr. Facil.*, **35**(6), 04021092. https://doi.org/10.1061/(ASCE)CF.1943-5509.0001652

Jin, S., Lee, S.E. and Hong, J.W. (2020), "A vision-based approach for autonomous crack width measurement with flexible kernel", *Automat. Constr.*, **110**, 103019. https://doi.org/10.1016/j.autcon.2019.103019

Jung, H.J., Lee, J.H., Yoon, S. and Kim, I.H. (2019), "Bridge Inspection and condition assessment using Unmanned Aerial Vehicles (UAVs): Major challenges and solutions from a practical perspective", *Smart Struct. Syst., Int. J.*, **24**(5), 669-681. https://doi.org/10.12989/sss.2019.24.5.669

Kang, D.H. and Cha, Y.J. (2022), "Efficient attention-based deep encoder and decoder for automatic crack segmentation", *Struct. Health Monitor.*, **21**(5), 2190-2205. https://doi.org/10.1177/14759217211053776

Kang, D., Benipal, S.S., Gopal, D.L. and Cha, Y.J. (2020), "Hybrid pixel-level concrete crack segmentation and quantification across complex backgrounds using deep learning", *Automat. Constr.*, **118**, 103291. https://doi.org/10.1016/j.autcon.2020.103291

Kim, H., Ahn, E., Cho, S., Shin, M. and Sim, S.H. (2017), "Comparative analysis of image binarization methods for crack identification in concrete structures", *Cement Concrete Res.*, **99**, 53-61. https://doi.org/10.1016/j.cemconres.2017.04.018

Kim, H., Lee, J., Ahn, E., Cho, S., Shin, M. and Sim, S.H. (2017), "Concrete crack identification using a UAV incorporating hybrid image processing", *Sensors*, **17**(9), p. 2052. https://doi.org/10.3390/s17092052

Lee, J.S., Hwang, S.H., Choi, I.Y. and Choi, Y. (2020), "Estimation of crack width based on shape sensitive kernels and semantic segmentation", *Struct. Control Health Monit.*, **27**(4), e2504. https://doi.org/10.1002/stc.2504

Liang, X., Du, X., Wang, G. and Han, Z. (2019), "A deep reinforcement learning network for traffic light cycle control", *IEEE Transact. Vehicul. Technol.*, **68**(2), 1243-1253. https://doi.org/10.1109/TVT.2018.2890726

Liu, P., Chen, A.Y., Huang, Y.N., Han, J.Y., Lai, J.S., Kang, S.C., Wu, T.H., Wen, M.C. and Tsai, M.H. (2014), "A review of rotorcraft Unmanned Aerial Vehicle (UAV) developments and applications in civil engineering", *Smart Struct. Syst., Int. J.*, **13**(6), 1065-1094. https://doi.org/10.12989/sss.2014.13.6.1065

Liu, W., Anguelov, D., Erhan, D., Szegedy, C., Reed, S., Fu, C.Y. and Berg, A.C. (2016), "SSD: Single shot multibox detector", *Proceedings of the 14th European Conference on Computer Vision–ECCV 2016*.

Liu, Z., Yao, C., Yu, H. and Wu, T. (2019), "Deep reinforcement learning with its application for lung cancer detection in medical Internet of Things", *Future Gener. Comput. Syst.*, **97**, 1-9. https://doi.org/10.1016/j.future.2019.02.068

Liu, Y.F., Nie, X., Fan, J.S. and Liu, X.G. (2020), "Image-based crack assessment of bridge piers using unmanned aerial vehicles and three dimensional scene reconstruction", *Comput.-Aided Civil Infrastr. Eng.*, **35**(5), 511-529. https://doi.org/10.1111/mice.12501

Long, J., Shelhamer, E. and Darrell, T. (2017), "Fully convolutional networks for semantic segmentation", *IEEE Transact. Pattern Anal. Mach. Intell.*, **2015**, 3431-3440.

Mnih, V., Kavukcuoglu, K., Silver, D., Rusu, A.A., Veness, J., Bellemare, M.G., Graves, A., Riedmiller, M., Fidjeland, A.K., Ostrovski, G. and Petersen, S. (2005), "Human-level control through deep reinforcement learning", *Nature*, **518**, 529-533. https://doi.org/10.1038/nature14236

Mnih, V., Kavukcuoglu, K., Silver, D., Graves, A., Antonoglou, I., Wierstra, D. and Riedmiller, M. (2013), "Play atari with deep reinforcement learning", *arXiv preprint arXiv*:1312.5602. https://doi.org/10.48550/arXiv.1312.5602

Mocanu, E., Mocanu, D.C., Nguyen, P.H., Liotta, A., Webber, M.E., Gibescu, M. and Slootweg, J.G. (2018), "On-line building energy optimization using deep reinforcement learning", *IEEE Transact. Smart Grid*, **10**(4), 3698-3708. https://doi.org/10.1109/TSG.2018.2834219

Ni, F., Zhang, J. and Chen, Z. (2019), "Zernike-moment measurement of thin-crack width in images enabled by dual-scale deep learning", *Comput. Aided Civil Infra.*, **34**, 367-384.

Ong, J.C., Ismadi, M.Z.P. and Wang, X. (2022), "A hybrid method for pavement crack width measurement", *Measurement*, **197**, 111260. https://doi.org/10.1016/j.measurement.2022.111260

Park, S.E., Eem, S.H. and Jeon, H. (2020), "Concrete crack detection and quantification using deep learning and structured light", *Constr. Build. Mater.*, **252**. https://doi.org/10.1016/j.conbuildmat.2020.119096

Payab, M., Abbasina, R. and Khanzadi, M. (2018), "A brief review and a new graph-based image analysis for concrete crack quantification", *Arch. Computat. Methods Eng.*, **26**, 347-365. https://doi.org/10.1007/s11831-018-9263-6

Peng, X., Zhong, X., Zhao, C., Chen, A. and Zhang, T. (2021), "A UAV-based machine vision method for bridge crack recognition and width quantification through hybrid feature learning", *Constr. Build. Mater.*, **299**, 123896. https://doi.org/10.1016/j.conbuildmat.2021.123896

Ribeiro, D., Santos, R., Shibasaki, A., Montenegro, P., Carvalho, H. and Calçada, R. (2020), "Remote inspection of RC structures using unmanned aerial vehicles and heuristic image processing", *Eng. Fail. Anal.*, **117**, 104813. https://doi.org/10.1016/j.engfailanal.2020.104813

Redmon, J. and Farhadi, A. (2018), "Yolov3: An incremental improvement", *arXiv preprint arXiv*:1804.02767. https://doi.org/10.48550/arXiv.1804.02767

Ren, Y., Huang, J., Hong, Z., Lu, W., Yin, J., Zou, L. and Shen, X. (2020), "Image-based concrete crack detection in tunnels using deep fully convolutional networks", *Constr. Build. Mater.*, **234**, 117367. https://doi.org/10.1016/j.conbuildmat.2019.117367

Ronneberger, O., Fischer, P. and Brox, T. (2015), "U-net:

Convolutional networks for biomedical image segmentation", *Proceedings of the 18th International Conference Medical Image Computing and Computer-Assisted Intervention–MICCAI 2015*.

Shan, B., Zheng, S. and Ou, J. (2015), "A stereovision-based crack width detection approach for concrete surface assessment", *KSCE J. Civil Eng*., **20**, 803-812. https://doi.org/10.1007/s12205-015-0461-6

Song, Y., Huang, Z., Shen, C., Shi, H. and Lange, D.A. (2020), "Deep learning-based automated image segmentation for concrete petrographic analysis", *Cement Concrete Res*., **135**, 106118. https://doi.org/10.1016/j.cemconres.2020.106118

Song, L., Sun, H., Liu, J., Yu, Z. and Cui, C. (2022), "Automatic segmentation and quantification of global cracks in concrete structures based on deep learning", *Measurement*, **199**, 111550. https://doi.org/10.1016/j.measurement.2022.111550

Sony, S., Dunphy, K., Sadhu, A. and Capretz, M. (2021), "A systematic review of convolutional neural network-based structural condition assessment techniques", *Eng. Struct*., **226**(1), 111347. https://doi.org/10.1016/j.engstruct.2020.111347

Tang, Y., Huang, Z., Chen, Z., Chen, M., Zhou, H., Zhang, H. and Sun, J. (2023), "Novel visual crack width measurement based on backbone double-scale features for improved detection automation", *Eng. Struct*., **274**, 115158. https://doi.org/10.1016/j.engstruct.2022.115158

Wang, W., Zhang, A., Wang, K.C., Braham, A.F. and Qiu, S. (2018), "Pavement crack width measurement based on Laplace's equation for continuity and unambiguity", *Comput.-Aided Civil Infrastr. Eng*., **33**(2), 110-123. https://doi.org/10.1111/mice.12319

Wiering, M.A., Van Hasselt, H., Pietersma, A.D. and Schomaker, L. (2011), "Reinforcement learning algorithms for solving classification problems", *Proceedings of 2011 IEEE Symposium on Adaptive Dynamic Programming and Reinforcement Learning* (*ADPRL*), Paris, France, April, pp. 91-96. https://doi.org/10.1109/ADPRL.2011.5967372

Yao, L., Dong, Q., Jiang, J. and Ni, F. (2020), "Deep reinforcement learning for long-term pavement maintenance planning", *Comput.-Aided Civil Infrastr. Eng*., **35**, 1230-1245. https://doi.org/10.1111/mice.12558

Zhong, X., Peng, X., Yan, S., Shen, M. and Zhai, Y. (2018), "Assessment of the feasibility of detecting concrete cracks in images acquired by unmanned aerial vehicles", *Automat. Constr*., **89**, 49-57. https://doi.org/10.1016/j.autcon.2018.01.005

Zhong, X., Peng, X., Chen, A., Zhao, C., Liu, C. and Chen, Y.F. (2021), "Debonding defect quantification method of building decoration layers via UAV-thermography and deep learning", *Smart Struct. Syst., Int. J*., **28**(1), 55-67. https://doi.org/10.12989/sss.2021.28.1.055

Zhou, Y. and Liu, T. (2019), "Computer vision-based crack detection and measurement on concrete structure", *J. Tongji Univ.: Natural Sci*., **47**(9), 1277-1285. https://doi.org/10.11908/j.issn.0253-374x.2019.09.007

HJ